



Adsorption of Alkali Blue, Metanil Yellow and Neutral Red dyes Using Copper (II) Oxide particles: Kinetic and Thermodynamic Studies

Ibrahim, M. A. * and Ibrahim, M. B.

Department of Pure and Industrial Chemistry, Faculty of Physical Sciences, Bayero University, P.M.B. 3011, BUK, Kano, Nigeria.

Email: mibrahim042@gmail.com, mbibrahim.chm@buk.edu.ng

ABSTRACT

Copper (II) oxide particles (CuO-Ps) was synthesized and used for the removal of Metanil Yellow (MY), Alkali Blue (AB) and Neutral Red (NR). The influence of variables such as contact time, dosage, temperature and agitation speed for the adsorption process were investigated using Batch Adsorption Method. The synthesized particles were characterized using UV-Visible spectroscopy with a broad peak of 273 nm indicating the change in colour of the CuO-Ps from blue to brownish black with the formation of CuO-Ps. FTIR were carried out to determine the functional groups present at the surface of the particle with functional groups such as –OH, C=C, C-H, C≡C detected. SEM analysis of the CuO-Ps was carried out. The changes in the morphology was observed which is due to the attachment of the dye molecules at the surface of the particles. The percentage removal and optimum contact time of MY, AB and NR were obtained as 70.7% at 25 min, 84.8% at 10 mins and 56.9% at 30 min respectively. Kinetics studies of all the dyes shows that adsorption process fits pseudo second order with the experimental values of q_e 2.844, 4.242 and 3.536 for NR, AB and MY respectively being closer to the calculated values of the q_e 2.739, 4.108 and 3.222 for NR, AB and MY respectively. Non linearity from Bangham's plot shows that both film and pore diffusion played an important role in all the three adsorption processes. Negative values of ΔH and ΔG revealed that the process was exothermic and feasible. Positive and Negative values for ΔS showed spontaneity of the process and decrease in randomness. Values of ΔH -6.70, -20.30 and -7.76 kJ/mol for AB, NR and MY, respectively confirmed the adsorption process as physical in nature. The results indicated that copper (II) oxide particles can be used as a low cost adsorbent for the removal of MY, AB and NR from aqueous solutions.

Keywords: Adsorption, CuO, FTIR, Kinetic, SEM, Thermodynamics, UV-Visible spectroscopy

INTRODUCTION

Most of the industries we have today release wastes upon their preparation and manufacturing stages. These waste substances either pollute air or land, or find their ways to enter aquatic systems. Water pollution has thus become a major worldwide concern for many decades, and this problem is getting increasingly serious as it causes many adverse effects including health concerns. It is claimed that typical pollutants in water systems are organic substances, dyes, pesticides and heavy metals, which cause detrimental effects to natural aquatic systems through retardation and death of living organisms it holds. The greater environmental awareness in both the public and regulator sphere in recent years has necessitated for effective treatment of industrial effluent. As such, there has been a great deal of research in finding low cost adsorbents for the removal of contaminants from wastewater (Ibrahim, 2011; Weihua, 2010; Vijayakumar *et al.* 2012)

Adsorption has shown exciting potential in removing pollutants, such as dyes and heavy

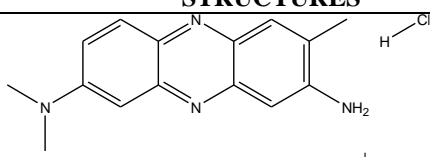
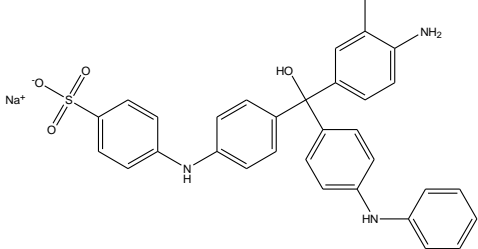
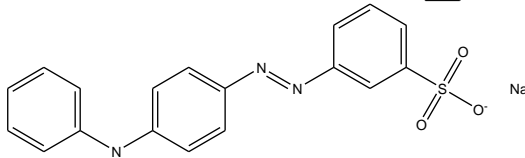
metals. Adsorbents can be from wastes such as Industrial waste product (Farouq and Yousef, 2015, Tahir *et al.* 2016), Treated Animal bone (Shehata, 2013), maize cob and saw dust (Ibrahim, 2013), Paliurus spina-christi Mill Frutis and Seeds (Selçuk *et al.* 2017), neem leave powder (Pandhare *et al.* 2013), and many others like nanoparticle (Ibrahim and Ibrahim, 2018; Luna *et al.* 2015; Taman *et al.* 2015). The reasons why adsorption has gained popularity in recent years lie in its having various attractive features such as abundance of materials which are low-cost, reusability, environmental friendliness, and low possibility of formation of harmful by-products as the pollutants are simply adsorbed onto the biomass in contrast to other methods employed in pollution control to clean the environment such as chemical, biological, filtration and thermal treatments, which are associated with many undesirable aspects.

This paper focused on the synthesis of copper (II) oxide particles and its uses for the aqueous phase removal of anionic dye Alkali Blue (AB), azo dye Metanil Yellow (MY) and a weak

cationic dye Neutral Red (NR). Also to study the kinetics and thermodynamics of the process as well

as optimization of some parameters.

Table 1: Dyes and Their Structures

DYES	STRUCTURES	REFERENCES
Neutral Red Dye		(Thiyab, 2008)
Alkali Blue Dye		(Gao and Mei, 2002)
Metanil yellow Dye		(Chiou and Chuang, 2004)

MATERIALS ANDMETHODS

Materials

The Instruments/Equipment's and Reagents used in these research are listed in Table 2 and3 respectively.

Table 2: Instrument/Equipments

S/N	Instruments/Equipment	Manufacturer/ Model
1	Analytical electronic weighing balance	FA2004
2	pH meter	Jenway 3510
3	Parkin Elmer UV-Visible spectrometer	Model Hitachi 2800
4	Fourier transform infrared spectroscopy	Cary 630; Agilent Technologies
5	Incubator shaker	Innova 4000 incubator shaker
6	Scanning Electron Microscope	SEM, Leica Stereoscan-440 interfaced with Phoenix EDX

Table 3: Reagents and their Percentage purity

S/N	Reagents	Percentage purity
1	Copper nitrate trihydrate (Cu(NO ₃),3H ₂ O)	99%
2	Sodium hydroxide (NaOH)	98%
3	Polyethylene glycol	--
4	Hydrochloric Acid (HCl)	38%
5	Alkali blue dye	80% Merck
6	Neutral red dye	90% Merck
7	Metanil Yellow dye	70% Merck

Synthesis of Copper (II) oxide Particles

The synthesis of Copper (II) Oxide particles was carried out by the use of method employed by Mayekar *et al.* (2014) with the use of Polyethylene glycol (PEG) instead of polyvinylpyrrolidone (PVP) due to its similar way of action which was to stabilize the aggregation of the metal ion. For the synthesis of the particles, 7.68 g of copper nitrate trihydrate was mixed with 2.4 g of polyethylene

glycol (PEG) and 200 cm³ of distilled water. The solution was stirred using magnetic stirrer and heated till it reached 60 °C. Once the desired temperature was reached, 1.0 M of sodium hydroxide solution and 1.0 M hydrochloric acid were added drop by drop to adjust the pH of the solution to 7.0. After then it was heated at 60 °C and stirred for two hours. Brownish black particles were formed. The mixture was centrifuged and

oven dried at 50 °C for 8 hrs to obtain copper (II) oxide particles.

CHARACTERIZATION OF SYNTHESIZED COPPER (II) OXIDE PARTICLES

Visual Inspection

In the process of synthesizing the copper (II) oxide particles, a colour change was observed from blue to brownish black. The copper (II) oxide particle obtained was characterized using UV-Visible spectroscopy, Fourier Transform Infrared Spectroscopy and Scanning Electron Microscopy.

UV-Visible Spectroscopy

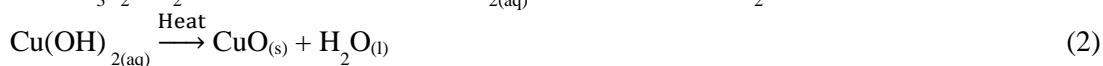
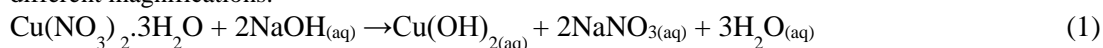
UV-Visible spectroscopy of the synthesized copper (II) oxide particles was carried out to determine the maximum absorption wavelength of the synthesized particles.

FT-IR Analysis of Copper (II) Oxide Particle Before and After Adsorption

FT-IR measurements of the copper oxide nanoparticles was carried out to identify the possible functional groups that may be responsible for the adsorption of Alkali Blue (AB), Neutral Red (NR) and Metanil Yellow (MY) dyes using FTIR-Cary 630 from Agilent technologies and the spectra was recorded in the wavelength interval 4000 to 500 cm⁻¹.

Scanning Electron Microscopy (SEM)

Scanning electron microscopy (SEM) gives image of a surface of a materials/specimens at a desired position and therefore displayed topographic/morphological picture with better resolution and depth of focus Eddy *et al.*, (2014). SEM was further carried out in order to ascertain the surface morphology of the synthesized copper (II) oxide particles. The images were taken at different magnifications.



CHARACTERIZATION OF COPPER (II) OXIDE PARTICLES

UV-Visible Studies on Copper (II) Oxide Particles

UV-Visible spectroscopy has proved to be a very useful technique for studying metal nanoparticles because the peak positions and shapes are sensitive to the particle size. In this work, characterization of copper (II) oxide particles using UV-spectrophotometer was carried in the range 200 to 750 nm, where a broad peak was observed at 273 nm which closely correspond to that of literature with Fardood and Ramazani (2016) reporting the change in colour of copper oxide nanoparticle at 262 nm. The absorption was due to colour rather than particle size. The absorption range for copper oxide particles was in

ADSORPTION STUDIES

Batch Adsorption Experiment

The influence of variables including, amount of adsorbent, contact time, temperature, agitation rate on the adsorptive removal of the dyes were all investigated in batch mode at room temperature (30 ± 3 °C). In each experiment, 100 cm³ of dyes in a 120 cm³ bottle was agitated and stirred at 300 rpm along with a fixed mass of the nanoparticles at constant temperature. The mixture was then filtered; and the filtrate was centrifuged (Ibrahim, 2013). The clear supernatant was used to determine the final concentration of the dyes spectrophotometrically using UV-Visible spectrophotometer (Hitachi 2800) at a predetermined corresponding λ_{max} of each dye; 581 nm for AB, 430 nm for MY and 455 nm for NR respectively. The experimental data at various times and temperature were fitted to different models to evaluate and calculate the kinetic and thermodynamic parameters for the adsorption process. The solution pH was adjusted by the addition of dilute aqueous solutions of 0.1 M HCl and 0.1 M NaOH.

RESULTS AND DISCUSSION

Visual Characterization

The preparation of copper (II) oxide particles involved stages. When copper nitrate tri hydrate solution was mixed with PEG the solution appeared light blue in colour. On adjusting the pH using 1.0 M NaOH and 1.0 M HCl, brown precipitates was formed. On heating the precipitate at a temperature of about 60 °C the colour changed to brownish black which indicated the formation of the copper (II) oxide particles as represented by equations 1 and 2.

the UV region of 200 – 400 nm in which no colour was observed.

Fourier Transform- Infrared (FT-IR) Characterization

FT-IR spectra of CuO-Ps and after adsorption with Alkali Blue, Metanil Yellow and Neutral Red were taken and compared with the CuO-Ps before adsorption to obtain information on the nature of the possible adsorbent-adsorbate interactions. The spectra of the samples showed the presence of several functional groups such as -OH, C≡C, C=C and C-H. The FT-IR spectra of the CuO-Ps both before and after adsorption with AB, MY & NR were shown in Table 2. They demonstrated that after the adsorption, shifting occurs both to higher and lower wave numbers. This shifting indicated that there were binding

processes taking place on the surfaces of the substrates (Stuart, 2004). Broad band of 3550-3200 cm^{-1} represented –OH groups, 3000-2850 cm^{-1} represented aliphatic C-H group, 2250-2100 cm^{-1} represented $\text{C}\equiv\text{C}$ group. The functional groups could act as chemical of binding agents where

hydroxyl group dissociate negatively charged active surface (Nale *et al.*, 2012). The changes in wave numbers in relation to energy showed little difference which indicated the adsorption process to be physical.

Table 2: FT-IR results of CuO-Ps both before and after adsorption with AB, MY & NR

Peaks	CuO-NPs $\bar{\nu}$ (cm^{-1})				Functional Group Assignment
	Before Adsorption	After Adsorption with			
		AB	MY	NR	
1	3420	3413	3402	3417	Bonded –OH
2	2880	2925	2925	2929	Aliphatic C-H group
3	2199	2177	2110	2113	$\text{C}\equiv\text{C}$ group
4	1599	1581	1592	1603	$\text{C}=\text{C}$ stretching
5	1350	1343	1328	1346	-OH bending
6	1097	1033	1037	1063	C-O stretching

Scanning Electron Microscopy (SEM)

Scanning Electron Microscopy provided further insights into the morphology and size of the copper (II) oxide particles. From the micrographs, it can be observed that various shapes of copper oxide nanoparticles have been produced, which appear as discrete particles forming large aggregates. The micrograph of the synthesized

nanoparticle corresponds to that of Aparna *et al.*, (2012) which revealed the agglomeration of the nanoparticles. The observations of such nanoparticles are an indication that there is interaction between the dye molecules and the adsorbent surface. The micrographs of the Particles before and after adsorption of the dyes are shown in Figure 1 (a-d).

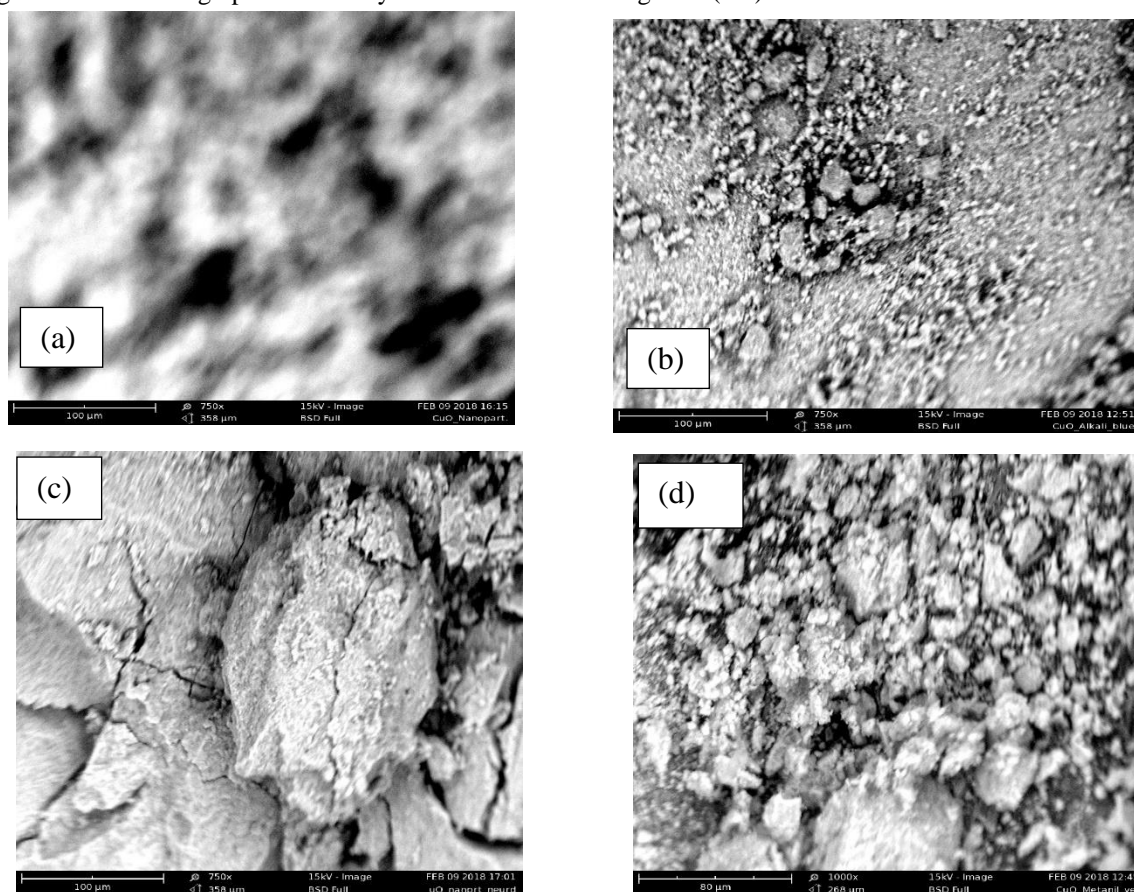


**Fig1: a. Micrograph of copper (II) oxide particles
c. After adsorption with Neutral red**

**b. After adsorption with Alkali blue
d. After adsorption with Metanil yellow**

Effect of Contact Time on Adsorption of MY, AB and NR

The results of adsorption with increasing contact time are presented in Fig. 2-4. The increase in contact time at 300 rpm stirring rate leads to enhancement in the dye adsorption. For MY about 70.7 % of the dye removal took place within the first 25 min (Fig. 2), which is due to high interaction between adsorbent and the dye, and also the availability of more active sites on the nanoparticles for the dye adsorption. Therefore, the equilibrium adsorption occurred at 25 min. This adsorption process shows lower percentage removal at higher time when compared to that of

Muthuraja and Kannan (2013), which they reported 85% removal after 20 min. For the adsorption of AB dye equilibrium was attained after 10 minutes with maximum removal percentage of about 84.8 % (Fig. 3). At a time above 10 minutes the percentage removal decreases which may due to fact that all the active site have been occupied. This is in agreement with Gao and Mei (2002). For the adsorption of NR dye, equilibrium was attained after 30 minutes with maximum removal percentage of about 56.9 % (Fig. 4). This is low when compared to 98 % removal reported by Elhami *et al.* (2012).

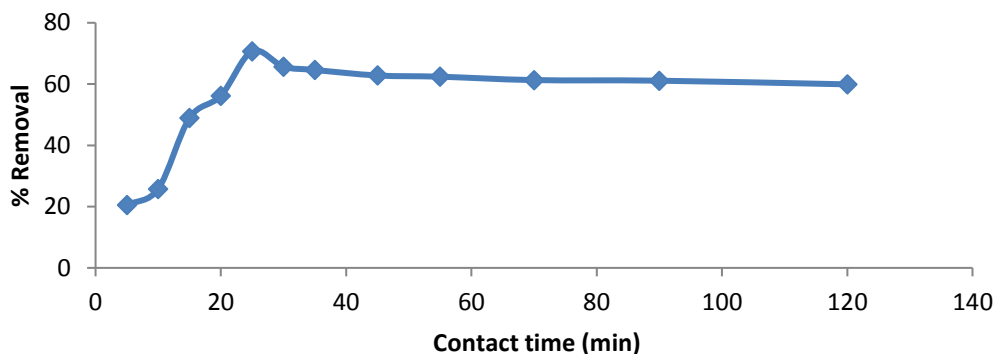


Fig 2: Effect of contact time on the removal of MY

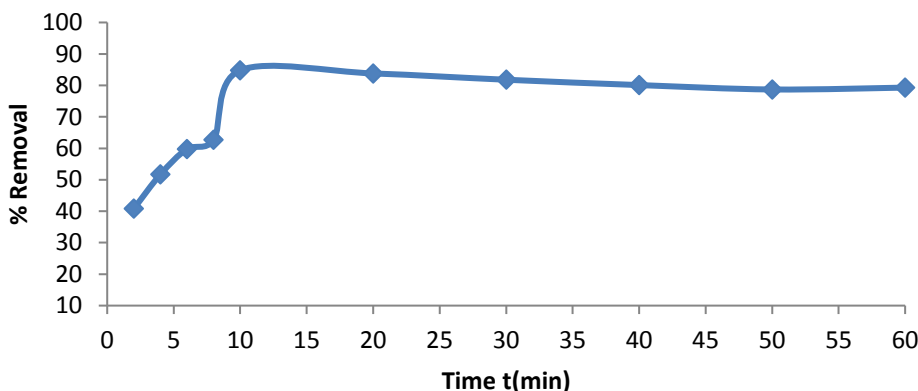


Fig 3: Effect of contact time on the removal of AB

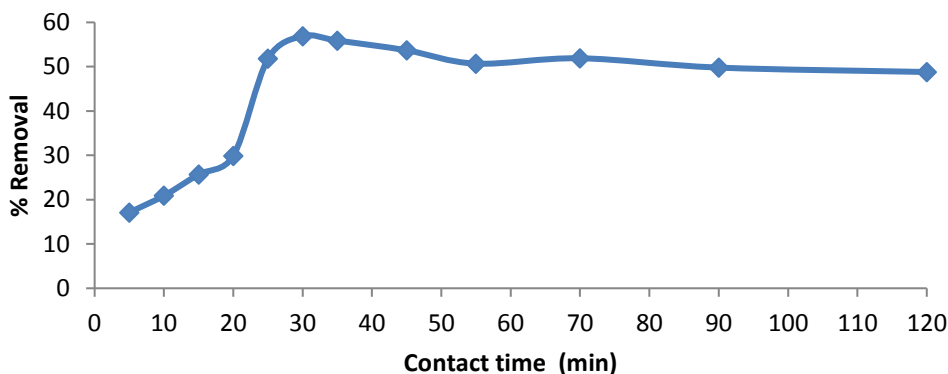


Fig 4: Effect of contact time on the removal of NR

Effect of Adsorbent Dosage

The effect of CuO-Ps dosage on the removal of MY, AB and NR are shown in Fig 5 respectively. For Metanil yellow (MY) dye, increase in the dosage from 0.1 g to 0.5 g led to decrease in the removal efficiency of the dye from 89.1 to about 81.0%. This may be attributed to the decrease in the total adsorption surface area available to the counter ionic dye, resulted in an overlapping or an aggregation of the adsorption sites (Nuengmacha *et al.* 2016). These result is in agreement with the results obtained by Tahir *et al.* (2016) and Vijayakumar *et al.* (2012).

However, for AB there was sharp rise in the percentage removal of the dye (from 48.4% to

85.6%) with increasing mass of the adsorbent from 0.1 to 0.4 g. At 0.5 g, there was slight decrease in removal percentage to about 85.1%. This may be due to the decrease in total surface area available resulting from overlapping or aggregation of adsorption sites as similarly observed by Nethaji *et al.* (2013). Similarly, for NR there is significant increase in adsorption (from 66.8 to 72.4%) with increasing mass of the adsorbent from 0.1 to 0.4 g. The adsorption process then decreased with further increase in the adsorbent dose to 0.5 g. The result for NR is in agreement with that of Kobiraj *et al.* (2012).

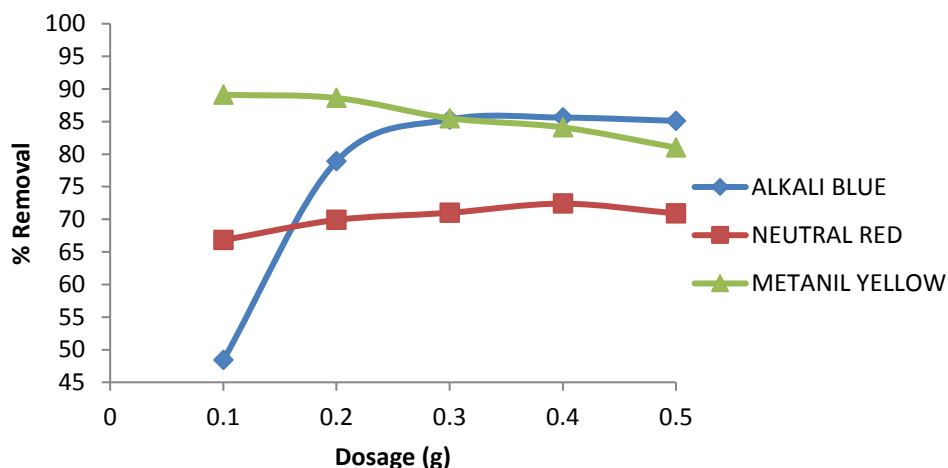


Fig 5: Effect of dosage on the removal of AB, NR & MY.

Effects of Agitation Speed

The effect of agitation speed was studied for AB, MY and NR dyes. The agitation speed studied are 100, 200 and 300 rpm. Result for all dyes in Fig. 6 shows that there is increase in percentage removed from 92.5 to 98.5% for MY, 90.4 to 92.8% for AB and 94.9 to 97.2% for NR respectively for agitation speed ranging from 100-

300 rpm. This shows that the dye removal increases with increase in agitation speed for all the three dyes. This may be due to the fact that proper contact between the dyes and active sites is developed when increasing the agitation speed, thus increase of the agitation speed improves the diffusion of the dyes towards the surface of the adsorbent (Alhaji and Tajun 2015).

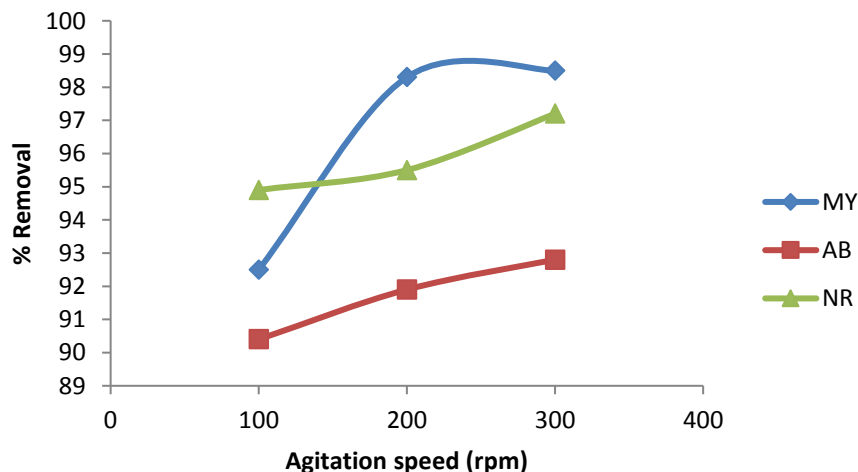


Fig 6: Effect of Agitation speed on the removal of AB, NR & MY.

Effects of Temperature

From Fig. 7, it could be observed that for all the dyes the percentage removal decreased with increase in temperature from 91.8 to 89.9% for AB, 98.6 to 93.9 for NR and 98.6 to 98.1% for MY. For all the three dyes there is decrease in percentage removal as the temperature is increased, this is because with increasing temperature, the attractive forces between adsorbent surface and dye molecules are weakened and the adsorption decreases Horsfall and Spiff, (2005).

AB, NR and MY dyes follow the same pattern as the temperature is increased the adsorption performance decreased which implies exothermic process. All the dyes due to the nature of the process which shows decrease in percent removal with increase in temperature implies that the adsorption process is physical in nature. The results of AB, NR and MY are in agreement with that of Bishnoi *et al.* (2004).

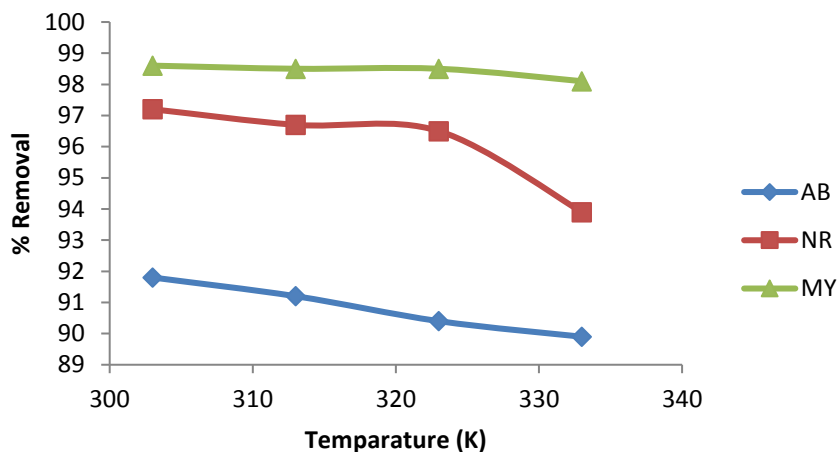


Fig 7: Effect of Temperature on the removal of AB, NR & MY.

ADSORPTION KINETICS

Pseudo-first-order equation

Pseudo first order integrated rate equation can be represented by equation (3):

$$\ln(q_e - q_t) = \ln q_e - Kt \quad (3)$$

where q_e is the equilibrium adsorption capacity (mg/g), q_t is the mass of dyes adsorbed at time t (mg/g), K is the first order rate constant (min^{-1}). A plot of $\ln(q_e - q_t)$ against t should give a slope and intercept of $\ln q_e$ and K giving a linear relationship for the applicability of the first order kinetic (Thilagan *et al.*, 2013). From Table 4, the q_e experimental and the q_e calculated values from pseudo first order are very far from each other for all the dyes. Also the calculated correlation

$$\frac{t}{q_t} = \frac{1}{K_2 q_e^2} + \frac{1}{q_e} t \quad (4)$$

A plot of t/q_t versus t should give a slope and intercept of $\frac{1}{q_e}$ and $\frac{1}{K_2 q_e^2}$ giving a linear relationship for the applicability of the second order kinetic (Thilagan *et al.*, 2013). As shown in Table 4, the q_e experimental and the q_e calculated values from the pseudo second- order kinetic model for all the dyes are very close to each other. The calculated correlation coefficients (R^2) are also close to unity for pseudo-second order kinetic than the other tested kinetic models. Therefore, the sorption can be approximated more appropriately by pseudo second order kinetic model for all the studied

coefficients (R^2) for all the three dyes are very low when compared to that of other kinetic models in the Table. This shows that the adsorptions of MY, AB and NR onto CuO-Ps do not follow the pseudo first-order kinetics.

Pseudo-second-order equation

Pseudo second order integrated rate equation is defined by equation (4):

adsorbates (Sumanjit *et al.*, 2012). The rate constant of pseudo-second order adsorption (k_2) obtained for NR was found to be lower than those computed for AB and MY (Table 3). This indicated that the uptake of NR onto CuO-Ps from aqueous solution was more rapid and favorable (Kalalagh *et al.*, 2011).

Elovich model

The Elovich equation generally used is expressed by equation (5):

$$q_t = \frac{1}{\beta} \ln(\alpha \beta) + \frac{1}{\beta} \ln(t) \quad (5)$$

q_t was plotted against $\ln(t)$. α is the initial adsorption rate ($\text{mg g}^{-1}\text{min}^{-1}$) and β is the desorption constant (g mg^{-1}) which are obtained from the slope and intercept of the plot (Gok *et al.*, 2008). The values of constants α and β are recorded in Table 4. For AB adsorption predominate desorption ($\alpha > \beta$), for NR desorption predominates adsorption ($\beta > \alpha$) and for MY both processes are taking place at about the same rate (α

$\approx \beta$). From the R^2 values it can be concluded that for all the dyes Elovich equation is not applicable.

Bangham's model

Bangham's equation was used to determine if pore diffusion is the only rate controlling step in the adsorption process or not. Bangham's model is given by equation (6);

$$\log \log \left[\frac{C_0}{C_0 - q_t m} \right] = \log \left[\frac{k_0 m}{2.303 V} \right] + \alpha \log t \quad (6)$$

where, C_0 is the initial concentration of the adsorbate in solution (mg L^{-1}), V is the volume of the solution (L), m is the adsorbent dose (g), q_t (mg g^{-1}) is the amount of adsorbate retained at time t , α (less than 1) and k_0 are the constants. (Chakrapani *et al.*, 2010). As such $\log \log [C_0/(C_0 - q_t m)]$ was plotted against $\log t$ for all three adsorbates. From the experimental data, the plot did not yield a desired linear fit in the double logarithmic plot for

all the three adsorbates. This indicated that the adsorption kinetics was not limited to pore-diffusion only. The values of k_0 , α and R^2 are presented in Table 4. The R^2 values are very low compared to other models tested. According to the result it can be concluded that both film and pore-diffusion played a significant role to different extend during the different stages of the adsorption process (Yaneva *et al.*, 2013).

Table 4: Kinetics parameters for adsorption of AB, NR and MY on CuO-Ps

Models	Kinetic Parameters	AB	NR	MY
Pseudo First Order	$q_{e,exp.}(\text{mg/g})$	4.242	2.844	3.536
	$q_{e,cal.}(\text{mg/g})$	1.061	1.192	1.007
	$k_1(\text{min}^{-1})$	0.0347	0.0161	0.0102
	R^2	0.359	0.410	0.234
Pseudo Second Order	$q_{e,cal.}(\text{mg/g})$	4.108	2.739	3.222
	$k_2(\text{g/mg.min})$	0.1746	0.0524	0.0726
	R^2	0.997	0.942	0.979
Elovich	$\alpha(\text{mg/g.min})$	20.035	0.598	1.484
	$\beta(\text{mg/g})$	1.762	1.576	1.551
	R^2	0.719	0.638	0.575
Bangham	$\alpha (\text{mL/g/L})$	0.188	0.013	0.332
	$k_0(\text{dm}^3 \text{g}^{-1})$	2.16×10^{-2}	1.95×10^{-2}	8.50×10^{-3}
	R^2	0.711	0.013	0.581

Conditions: ($C_0 = 10\text{mg/L}$, $m = 0.2 \text{ g}$, $T = 303\text{K}$)

Adsorption Thermodynamics

Thermodynamic considerations of an adsorption process are necessary to conclude whether the process is spontaneous or not. The Gibb's free energy change, ΔG , is an indication of spontaneity of a reaction and therefore is an important criterion

for spontaneity. Both enthalpy (ΔH) and entropy (ΔS) factors must be considered in order to determine the Gibb's free energy of the process. Change in Gibb's energy can be defined by equations 7 and 8;

$$\Delta G = -RT \ln K \quad (7)$$

$$\Delta G = \Delta H - T \Delta S \quad (8)$$

Where ΔH is the enthalpy change, ΔS is the entropy change and T is the absolute temperature

and K is the equilibrium constant of adsorption. Combining these equations we get equation (9):

$$-RT \ln K = \Delta H - T\Delta S \quad (9)$$

which simplifies to Van't-Hoff's equation

$$\ln K = \frac{\Delta S}{R} - \frac{\Delta H}{RT} \quad (10)$$

$\ln K$ was plotted against $1/T$ yields a straight line graph with intercept as $\frac{\Delta S}{R}$ and slope equals to $\frac{\Delta H}{R}$. From the slope and intercept values of ΔH and ΔS will be calculated and both the two will be substituted into the equation $\Delta G = \Delta H - T\Delta S$ to determine the Gibbs free energy change of the reaction (ΔG) at different temperatures.

From the values obtained (Table 5), the Gibbs free energy (ΔG) is the basic criterion of spontaneity and the negative values of ΔG at different temperatures (303–333 K) for all the three dyes reflect on the feasibility of the process. The adsorption of all the dyes from aqueous solution onto the CuO-Ps was spontaneous in nature.

The change of free energy for physisorption is usually between -20 and $0 \text{ kJ}\cdot\text{mol}^{-1}$, whereas chemisorptions are in the range of -80 to $400 \text{ kJ}\cdot\text{mol}^{-1}$ (Nejati *et al.* 2011; Zarrouk *et al.* 2011). The ΔG values of -6.102 to $-6.043 \text{ kJ}\cdot\text{mol}^{-1}$, -9.326 to $-8.031 \text{ kJ}\cdot\text{mol}^{-1}$ and -10.800 to $-11.101 \text{ kJ}\cdot\text{mol}^{-1}$ for AB, NR and MY respectively suggest that the adsorption is physical in nature.

The negative values of ΔH for adsorption of AB, NR and MY confirmed that the adsorption is exothermic in nature. The magnitude of ΔH may also give an idea about the type of the sorption process.

Typically, adsorption enthalpy of physisorption is lower than 40 kJ/mol , while that of chemisorptions may approach 100 kJ/mol (Zubairu *et al.*, 2011). In this work, ΔH values of -6.700 , -20.30 and $-7.764 \text{ kJ mol}^{-1}$ for AB, NR and MY respectively are all below 40 kJ mol^{-1} and hence confirming the process to be physisorption.

Moreover, positive value of ΔS for adsorption of MY dye on CuO-Ps suggested that the process was spontaneous (Ibrahim, 2012). While the negative value of entropy change (ΔS) for AB and NR dye on CuO-Ps also implied a decrease in randomness/disorder at the solid/liquid interface during the adsorption process (Saha and Chowdhury, 2011). These indicated that the final entropy of the dye molecules on the adsorbent surface was less than the initial entropy in the aqueous solution which resulted to orderliness of the dye molecules at the surface of the adsorbent.

Table 5: Thermodynamic parameters for adsorption of AB, NR and MY on CuO-Ps

Dyes	ΔG (kJ/mol)				ΔH (kJ/mol)	ΔS (kJmol ⁻¹ K ⁻¹)
	$\Delta G = \Delta H - T\Delta S$					
	303	313	323	333		
AB	-6.102	-6.082	-6.062	-6.043	-6.700	-0.002
NR	-9.092	-8.722	-8.352	-7.982	-20.300	-0.037
MY	-10.801	-10.901	-11.001	-11.101	-7.764	0.010

Conditions: ($C_0 = 30, 100$ & 200 mg/L for AB, MY & NR, $m = 0.1 \text{ g}$ for AB, 0.4 g for MY & NR. $\text{pH} = 5.30, 5.09$ & 3.37 for AB, MY & NR respectively).

CONCLUSION

In conclusion, copper (II) oxide particles was successfully synthesized using co-precipitation method. The formation of CuO-Ps was confirmed by Uv-Vis showing absorbance at about 273 nm due to colour change, SEM and FT-IR was also tested to see the effect of adsorption before and after based on morphology and functional groups present. The particles were found to be active in removal of dyes (MY, AB and NR) in aqueous solution with contact time of $10, 25$ and 30 min obtained for AB, MY and NR, respectively. The adsorption process was well suited to the pseudo-second-order kinetic model with their experimental and theoretical q_e being closer to each other. Similarly, the R^2 value fitted better to pseudo

second order model. Result from Bangham's model showed that both film and pore diffusion played an important role in all the three adsorption processes. Effect of agitation speed showed high percentage removal at higher agitation speed. Effect of dosage, and temperature were also found to be among the factors that influenced removal rates. Negative values of ΔG showed the process to be feasible, Negative values of ΔH indicates an exothermic process for all the dyes. This finding therefore, suggested that copper (II) oxide particles can serve as cheap, readily available adsorbent for the removal of MY, AB and NR dyes from aqueous solutions and paves way for environmental remediation.

REFERENCES

- Alhaji N.M.I. and Tajun K.M. (2015). Optimization and Kinetic Study For The Removal Of Chromium (VI) Ions By Acid Treated Sawdust Chitosan Composite Beads. *International Research Journal Of Pure And Applied Chemistry*. 5. 160-176.
- Aparna Y., Rao K .V., and Subbarao P. S.(2012). Preparation and Characterization of CuO Nanoparticles by Novel Sol-Gel Technique, *Journal of Nano- and Electronic physics*, 4(3), 03005(1-4).
- Bishnoi N. R., Pant A., and Garima (2004). Biosorption of copper from aqueous solution using algal biomass, *Journal of scientific and Industrial research*, 63;813-816.
- Chakrapani CH., Babu CH. S., Vani K.N.K and Rao S. (2010). Adsorption Kinetics for the removal of fluoride from aqueous solution by Activated carbon adsorbents derived from the peels of selected citrus fruits, *E-Journal of Chemistry*, 7(S1):S419-S427.
- Chiou M.S. And Chuang G. S (2004). Competitive Adsorption Of Dye Metanil Yellow And RB15 In Acid Solutions On Chemically Cross-Linked Chitosan Beads, *Chemosphere* (62) 731–740.
- Eddy N. O., Udofia I., Uzairu A., Odiongenyi A.O., and Obadimu C., (2014). Physicochemical, Spectroscopic and Rheological Studies on *Eucalyptus Citriodora* (EC) Gum, *Journal of Polymer and Biopolymer Physics Chemistry*, 2(1), 12-24.
- Elhami S., Faraji H. And Taheri M. (2012). Removal Of Neutral Red Dye From Water Samples Using Adsorption On Bagasse And Sawdust, *Journal of the Chemical Society of Pakistan*, 34 (2): 269-273.
- Fardood S. T., and Ramazani A. (2016). Green synthesis and characterization of copper oxide nanoparticles using coffee powder extract, *Journal of Nanostructure*, 6(2); 167-171.
- Farouq R. And Yousef N. S. (2015). Equilibrium and Kinetics Studies Of Adsorption Of Copper(II) Ions On Natural Biosorbent, *International Journal Of Chemical Engineering And Applications*, 6(5) : 319-324
- Gao H. W., and Mei H.D., (2002). Langmuir Aggregation Of Alkali Blue 6B In Proteins: Study And Application, *Macromolecular Bioscience*, 2(6): 280-285
- Gok O., Ozcan, A, Erdem, B. A. And Ozcan, S.(2008). Prediction Of The Kinetics, Equilibrium And Thermodynamic Parameters Of Adsorption Of Copper(II) Ions Onto 8-Hydroxy Quinolone Immobilized Bentonite. *Colloids and Surfaces A: Physicochemical Engineering Aspects*, 31: 174–185.
- Horsfall Jr. M. and Spiff A. I. (2005). Effects Of Temperature On The Sorption Of Pb²⁺ And Cd²⁺ From Aqueous Solution By *Caladium Bicolor* (Wild Cocoyam) Biomass, *Electronic Journal Of Biotechnology*, 8(2) : 162-169.
- Ibrahim, M.A. and Ibrahim M.B. (2018). Isotherm and Kinetic Studies on the Adsorptive Removal of Metanil Yellow and Neutral Red Dyes Using Copper Oxide Nanoparticles. *Chemical Science International Journal*, 22(4): 1-10.
- Ibrahim M. B. (2013). Thermodynamics And Adsorption Efficiencies Of Maize Cob And Sawdust For The Remediation Of Toxic Metals From Wastewater, *Journal Of Geoscience And Environment Protection*, 1(2) 18-21.
- Ibrahim M.B. (2011). Removal Of Toxic Metals From Aqueous Solution By Sawdust, *Bayero Journal Of Pure And Applied Sciences*, 4(1): 88 – 93.
- Ibrahim M.B. (2012). Coal and Zea Mays Cob Waste as Adsorbents For Removal Of Metallic Ions From Wastewater, *Bayero Journal Of Pure And Applied Sciences*, 5(2): 41 – 46.
- Kalalagh S. S., Babazadeh H., Nazemi A.H., And Manshoury M. (2011). Isotherm And Kinetic Studies On Adsorption Of Pb, Zn And Cu By Kaolinite, *Caspian Journal of Environmental Science*, 9(2) :243-255.
- Kobiraj R., Gupta N., Kushwaha A. K., and Chattopadhyaya M. C. (2012). Determination Of Equilibrium, Kinetic And Thermodynamic Parameters For The Adsorption Of Brilliant Green Dye From Aqueous Solutions Onto Eggshell Powder, *Indian Journal Of Chemical Technology*, 19: 26-31.
- Luna, I.Z., Hilary, L.N., Chowdhury, A.M.S., Gafur, M.A., Khan, N. and Khan, R.A. (2015) Preparation And Characterization Of Copper Oxide Nanoparticles Synthesized Via Chemical Precipitation Method. *Open Access Library Journal*, 2: E1409.
- Mayekar J. Dhar V. and Radha S., (2014). Synthesis Of Copper Oxide Nanoparticles Using Simple Chemical Route, *International Journal Of Scientific and Engineering Research* (5) 10: 928-930
- Muthuraja K. and Kannan C. (2013). Kinetic and Isotherm Studies Of Removal Of Metanil Yellow Dye On Mesoporous Aluminophosphate Molecular Sieves, *Chemical Science Transactions*, 2(S1), S195-S201.
- Nale, B. Y., Kagbu, J. A., Uzairu A., Nwankwere E. T., Saidu S. and Musa H. (2012). Kinetic and Equilibrium Studies of the Adsorption of Lead(II) and Nickel(II) ions from aqueous solutions on Activated Carbon

- Prepared from Maize Cob, *Der Chemica Sinica*, 3(2):302-312.
- Nejati K., Rezvani Z., Mansurfar M., Mirzaee A., And Mahkam M. (2011). Adsorption Of Metanil Yellow Azoic Dye From Aqueous Solution Onto Mg-Fe-NO₃ Layered Double Hydroxide. *Zetschrift fur An organische und Allgemeine Chemie*, 637: 1573–1579.
- Nethaji S., Sivasamy A. And Mandal A. B. (2013). Adsorption Isotherms, Kinetics And Mechanism For The Adsorption Of Cationic And Anionic Dyes Onto Carbonaceous Particles Prepared From Juglans Regia Shell Biomass, *International Journal of Environmental Science and Technology*, 10:231–242
- Nuengmatcha, P., Mahachai, R. And Chanthai, S. (2016). Adsorption Capacity Of The As-Synthetic Graphene Oxide For The Removal Of Alizarin Red S Dye From Aqueous Solution. *Oriental Journal of Chemistry*, 32(3); 1399-1410.
- Pandhare G. G., Trivedi N., And Dawande S. D., (2013). Adsorption Of Color From A Stock Solution Using Neem Leaves Powder As A Low-Cost Adsorbent, *International Journal Of Engineering Sciences & Emerging Technologies*, 2(5) : 97-103
- Saha P. and Chowdhury S. (2011). Insight Into Adsorption Thermodynamics, *Thermodynamics, Intech Open*, 16: 349-366
- Selçuk N. C., Kubilay S., Savran A. and Kul A. R. (2017). Kinetics And Thermodynamic Studies Of Adsorption Of Methylene Blue From Aqueous Solutions Onto *Paliurus Spina-Christi* Mill. Frutis And Seeds. *Journal Of Applied Chemistry*, 10(5): Ver. I, 53-63
- Shehata A. M. A. (2013). Removal Of Methylene Blue Dye From Aqueous Solutions By Using Treated Animal Bone As A Cheap Natural Adsorbent, *International Journal Of Emerging Technology And Advanced Engineering*, 3(12): 507-514.
- Stuart, B. (2004) *Infrared spectroscopy Fundamentals and Applications*. Analytical Techniques in the sciences. John Wisley and Sons Ltd. P 76-80.
- Sumanjit, Rani S., and Mahajan R.K. (2012). Equilibrium, Kinetics And Thermodynamic Parameters For Adsorptive Removal Of Dye Basic Blue 9 By Ground Nut Shells And Eichhornia. *Arabian Journal Of Chemistry*, 1-14.
- Tahir H., Sultan M., Akhtar N., Hameed U. And Abid T., (2016). Application Of Natural And Modified Sugar Cane Bagasse For The Removal Of Dye From Aqueous Solution, *Journal Of Saudi Chemical Society*, 20, S115–S121.
- Taman R, Ossman ME, Mansour MS, Farag HA (2015) Metal Oxide Nano-Particles as An Adsorbent For Removal Of Heavy Metals. *Journal Of Advanced Chemical Engineering*, 5: 125: 1-8
- Thilagan J., Gopalakrishnan S. And Kannadasan T. (2013). Adsorption Of Copper (II) Ions In Aqueous Solution By Chitosan Immobilised On Red Soil: Isotherms, Kinetics And Mechanism, *International Journal Of Pharmaceutical And Chemical Sciences*, 2(2), 1055-1066.
- Thiyab R. M. (2008). Removal Of Neutral Red Dye From Aqueous Solution By Adsorption Onto Rice Bran, *National Journal Of Chemistry*, 31:400-414.
- Vijayakumar G., Tamilarasan R. And Dharmendirakumar M. (2012). Adsorption, Kinetic, Equilibrium And Thermodynamic Studies On The Removal Of Basic Dye Rhodamine-B From Aqueous Solution By The Use Of Natural Adsorbent Perlite, *Journal of Material and Environmental Science*, 3(1); 157-170
- Weihua Z., Hongjuan Bai, Ke Li, Xiaolan Shi And Runping Han (2010). Use Of Oxalic Acid-Modified Rice Husk For The Adsorption Of Neutral Red From Aqueous Solutions, *Adsorption Science & Technology*, 28 (7): 641-656.
- Yaneva Z.L., Koumanova B.K., and Allen S.J. (2013). Applicability comparison of different kinetic/diffusion models for 4-nitrophenol sorption on *Rhizopus oryzae* dead biomass, *Bulgarian Chemical Communications*, 2:161-168.
- Zarrouk A., Hammouti B., Zarrok H., Al-Deyab S.S. And Messali M. (2011). Temperature Effect, Activation Energies And Thermodynamic Adsorption Studies Of L-Cysteine Methyl Ester Hydrochloride As Copper Corrosion Inhibitor In Nitric Acid 2M, *International Journal of Electrochemical Science*, 6 : 6261 – 6274.
- Zubairu S.M.J., Uzairu A., Iyun J.F, Abechi S.E. And Okunola J.O. (2011). Methylene Blue Adsorption From Glycerol Solution Onto The Acicular Habit Of □- Goethite, *Bulletin of the Chemical Society of Ethiopia*, 25(1); 25-35.